Antiviral Research 96 (2012) 280–287

Contents lists available at SciVerse ScienceDirect

Antiviral Research

journal homepage: www.elsevier.com/locate/antiviral

Crucial role of the N-glycans on the viral E-envelope glycoprotein in DC-SIGN-mediated dengue virus infection

Marijke M.F. Alen, Kai Dallmeier, Jan Balzarini, Johan Neyts, Dominique Schols *

Laboratory of Virology and Chemotherapy, Rega Institute for Medical Research, University of Leuven, Minderbroedersstraat 10, B-3000 Leuven, Belgium

ARTICLE INFO

Article history:
Received 6 June 2012
Revised 16 October 2012
Accepted 21 October 2012
Available online 31 October 2012

Keywords:
Dengue virus
DC-SIGN
Dendritic cells
Carbohydrate binding agent
N-glycan
Viral entry

ABSTRACT

We generated in the mosquito cell line C6/36 a dengue virus (DENV) resistant to *Hippeastrum* hybrid agglutinin (HHA), a carbohydrate-binding agent (CBA). The genotype and phenotype were characterized of the HHA resistant (HHA^{res}) DENV compared to the wild-type (WT) DENV. Sequencing the structural proteins of HHA^{res} resulted in two mutations, N67D and T155I, indicating a deletion of both N-glycosylation sites on the viral envelope E-glycoprotein. The HHA^{res} DENV could replicate in mammalian and mosquito cells that are lacking dendritic cell-specific intercellular adhesion molecule 3-grabbing non-integrin (DC-SIGN) expression. In contrast, DC-SIGN expressing human cells namely monocyte-derived dendritic cells as well as DC-SIGN-transfected cells were no longer susceptible to HHA^{res} DENV. This demonstrates a crucial role of the N-glycans in the E-glycoprotein in the infection of dendritic cells, which constitute primary target cells of DENV during viral pathogenesis in the human body.

1. Introduction

Dengue virus (DENV) is one of the most important emerging mosquito-borne viruses in tropical and subtropical countries. Following the bite of an infected mosquito, immature dendritic cells (DC) in the skin are believed to be the first target cells during DENV infection (Wu et al., 2000). Dendritic cell-specific intercellular adhesion molecule 3-grabbing non-integrin (DC-SIGN), a transmembrane calcium-dependent carbohydrate-binding receptor, is present on DC and can interact with the envelope proteins of several viruses such as human immunodeficiency virus (HIV) gp120 (Geijtenbeek et al., 2000) and DENV E-glycoprotein (Navarro-Sanchez et al., 2003; Tassaneetrithep et al., 2003; Lozach et al., 2005; Pokidysheva et al., 2006; Alen et al., 2009).

Previously, we demonstrated that DC-SIGN expression renders cells sensitive for DENV infection (Alen et al., 2009). DC-SIGN might be an important target for antiviral therapy, because it plays an initial role in virus transmission and infection. The DC-SIGN related receptor, L-SIGN, can also interact efficiently with DENV. L-SIGN is mainly expressed by endothelial liver cells which are also an important target for DENV (Seneviratne et al., 2006; Zellweger et al., 2010). Recently, carbohydrate-binding agents (CBAs) isolated from plants, i.e., *Hippeastrum hybrid* (HHA), *Galanthus nivalis* (GNA) and *Urtica dioica* agglutinin (UDA), have been shown to inhibit the interaction between HIV and DC-SIGN expressing cells (Balzarini et al., 2007). HHA, GNA and UDA were also found to dose-dependently inhibit the interaction between all four serotypes of DENV and DC-SIGN in Raji/DC-SIGN$^+$ cells and in monocyte-derived DC (MDDC) (Alen et al., 2009, 2011). Binding assays revealed that the CBAs do not interact with cellular membrane proteins such as DC-SIGN, but that they interact directly with the glycosylated envelope proteins of DENV, preventing the binding of DENV to DC-SIGN and subsequently preventing viral entry and infection (Alen et al., 2011). Here, we characterized the molecular target epitope of the CBAs by the generation of a HHA-resistant (HHA^{res}) DENV in mosquito cells by gradually increasing the concentration of HHA. We further characterized the mutant virus phenotypically and genotypically by respectively plaque formation and sequence analysis. We sequenced the viral genome encompassing the structural core (C), pre-membrane (prM) and envelope (E) proteins of DENV. The M-protein is expressed as a glycosylated precursor prM (~165 amino acids) which is attached to the E-protein until the viral particle is maturated. It is assumed that the prM protein assists in the folding and the trafficking of the E-protein during viral particle synthesis. After cleavage of the pr peptide, mature virions are formed and secreted together with the pr peptide (Rodenhuis-Zybert et al., 2010). The E-protein (~495 amino acids) is important in receptor binding and the induction of an immune response. The E-protein has two potential glycosylation sites: asparagines 67 (Asn67) and Asn153. Glycosylation at Asn153 is

* Corresponding author. Tel.: +32 16 337341; fax: +32 16 337340.
E-mail addresses: Marijke.Alen@rega.kuleuven.be (M.M.F. Alen), KaiHenrik.Dallmeier@rega.kuleuven.be (K. Dallmeier), Jan.Balzarini@rega.kuleuven.be (J. Balzarini), Johan.Neyts@rega.kuleuven.be (J. Neyts), Dominique.Schols@rega.kuleuven.be (D. Schols).

0166-3542/$ - see front matter © 2012 Elsevier B.V. All rights reserved.
http://dx.doi.org/10.1016/j.antiviral.2012.10.007

conserved in flaviviruses, with the exception of Kunjin virus (Scherret et al., 2001) and is located near the fusion peptide in domain II (Rey et al., 1995; Modis et al., 2003). Glycosylation at Asn67 is unique for DENV (Rey et al., 1995). Generally, the function of glycosylation of surface proteins is proper folding of the protein, trafficking in the endoplasmic reticulum, interaction with receptors and influencing virus immunogenicity (Vigerust and Shepherd,2007). We used the HHA^{res} DENV to elucidate the antiviral target (i.e., glycans on DENV E-glycoprotein) of several novel DENV entry inhibitors.

2. Materials and methods

2.1. Cell lines

All cell cultures were maintained at 37 °C in a humidified, CO_2-controlled atmosphere, except for C6/36 mosquito cells (isolated from *Aedes albopictus*; ATCC CRL-1660), which were maintained at 28 °C in the absence of CO_2. C6/36 cells were grown in Minimum Eagle's Medium (MEM) (Invitrogen, Merelbeke, Belgium) supplemented with 10% fetal bovine serum (FBS) (Hyclone, Perbio Science, Aalst, Belgium), 0.01 M HEPES buffer (Invitrogen), non-essential amino acids (Invitrogen), 2 mM L-glutamine (Invitrogen), 100 units/ml penicillin and 100 units/ml streptomycin (Invitrogen). Raji/DC-SIGN$^+$ cells were constructed by Geijtenbeek et al. (2000) and were kindly provided by Dr. L. Burleigh (Pasteur Institute, Paris, France). The plasmid containing L-SIGN cDNA was a kind gift of Dr. Stefan Pöhlmann (Institute for Clinical and Molecular Virology, Erlangen, Germany) (Pöhlmann et al., 2001) and were used for transfection experiments with L-SIGN cDNA to generate stable cell lines expressing the L-SIGN receptor. Raji/L-SIGN$^+$ cells were constructed using Amaxa Nucleofection electroporation system (Lonza, Cologne, Germany). Raji/0 and Raji/DC-SIGN$^+$ cell lines were cultivated in RPMI-1640 medium supplemented with 10% FBS and 2 mM L-glutamine and if L-SIGN was expressed 0.2 μg/ml geneticin was added. African green monkey kidney cells (Vero cells; ATCC CCL-81) were grown in MEM (Invitrogen,) supplemented with 10% FBS, 2 mM L-glutamine and 0.075% sodium bicarbonate (Invitrogen). Human hepatoma cells (Huh-7), kindly provided by Dr. R. Bartenschlager, and baby hamster kidney cells (BHK-21 cells; ATCC CCL-10) were grown in Dulbecco's Modified Eagle Medium (DMEM) supplemented with 10% FBS and 0.01 M HEPES buffer.

2.2. Isolation and differentiation of MDDC from human PBMCs

MDDC were isolated as described previously (Alen et al., 2011). Briefly, buffy coat preparations from healthy donors were obtained from the Blood Bank in Leuven, Belgium. Human peripheral blood mononuclear cells (PBMCs) were first isolated by density gradient centrifugation over Lymphoprep (Nycomed, Oslo, Norway). PBMCs were gently rotated at 4 °C to form aggregates of monocytes. After sedimentation of the monocytes, the pellet was grown in RPMI culture medium supplemented with or without 25 ng/ml IL-4 and 50 ng/ml GM-CSF (Peprotech, London, United Kingdom). After 5 days, IL-4 and GM-CSF differentiated monocytes into immature MDDC as analyzed by various cellular markers, such as DC-SIGN, mannose receptor, CD1a, CD11b, CD14, CD40, CD80, CD83 and CD86 by flow cytometry (Alen et al., 2011).

2.3. Viruses and selection of HHA-resistant virus

Dengue virus (DENV) serotype 2 laboratory-adapted New Guinea C (NGC) strain was kindly provided by Dr. V. Deubel (formerly Institut Pasteur, Lyon, France). DENV wild-type (WT) was propagated in C6/36 cells. Supernatant containing virus was harvested 5 days post infection and stored at −80 °C.

HHA-resistant DENV-2 (HHA^{res}) was generated in one HHA selection experiment by passaging a 1–20 dilution of the supernatant of HHA-exposed DENV-infected C6/36 mosquito cells (2×10^6 cells) every 3–4 days to fresh uninfected cells in the presence of gradually increasing concentrations of HHA. The drug resistance selection schedule is depicted in Fig. 1. After 14 passages (~7 weeks of cell culture), virus was recovered that could replicate in the presence of 400 nM of HHA, that is at a concentration ~10-fold higher than the EC_{50} for inhibition of DENV-2 replication in C6/36 cells. Titer of WT and HHA^{res} DENV was determined in a plaque assay using BHK-21 cells.

2.4. Plaque assay

Five 10- or 5-fold serial dilutions were made of WT and HHA^{res} DENV respectively, into 6-well plates containing a confluent monolayer of BHK-21 cells. Following an incubation of 4 h, the cells were washed 3 times with culture medium and overlaid with a solution containing 0.5% Avicel® (Matrosovich et al., 2006) and medium, supplemented with 2% FBS and 0.01 M HEPES buffer in a ratio 1:1. Avicel restricts the spread of virus in cell culture. After one week of culture, the cells were washed with PBS, fixed with 70% ethanol and stained with 1% methylene blue solution to visualize the plaques. Plaques were counted to determine the number of plaque forming units per milliliter supernatant (PFU/ml).

2.5. Test compounds

The mannose-specific plant lectins from *Hippeastrum hybrid* (HHA) (50 kDa), *G. nivalis* (GNA) (50 kDa) and the N-acetylglucosamine (GlcNAc)-specific plant lectin from *U. dioica* (UDA) (8.7 kDa) were derived and purified from these plants as described previously (Van Damme et al., 1987,1991). Pradimicin-S (PRM-S, 910 Da) was isolated from *Actinomadura* sp. TP-A0020 as described previously (Saitoh et al., 1993). Ribavirin (Virazole; RBV, 244 Da) was purchased from ICN Pharmaceuticals (Costa Mesa, CA). The doxorubicin derivate SA-17 (653 Da) was synthesized and kindly provided by Dr. F. Sztaricskai (Sztaricskai et al., 2005).

2.6. Population sequencing of HHA^{res} DENV

The genotype of the HHA^{res} DENV-2 was determined by sequencing ~3000 nucleotides of the viral genome encompassing the structural core (C), pre-membrane (prM) and envelope (E) proteins as described previously (Christenbury et al., 2010). Viral RNA was extracted from supernatants according to the manufacturer's instructions (Nucleospin RNA Virus Kit, Macherey–Nagel, Düren, Germany), reverse transcribed using SuperScript III Reverse Transcriptase (Invitrogen) and amplified using the KAPA HiFi HotStart PCR ReadyMix (KAPA Biosystems, Eke, Belgium) and primers #491 and #524 (Table 1). First strand cDNA synthesis was performed at 55 °C for 60 min and subsequent amplification according a PCR profile of 5 min at 95 °C for initial activation, followed by 30 cycles of 20 s at 98 °C, 15 s at 65 °C and 90 s at 72 °C each plus a final elongation of 10 min at 72 °C after cycling. Amplification products were gel-purified (Qiagen, Venlo, The Netherlands) and sequenced using a set of nested primers listed in Table 1 and the BigDye Terminator sequencing system (Applied Biosystems, Nieuwerkerk aan den IJssel, The Netherlands). The sequences were compared with WT DENV-2 passaged in parallel in the absence of drug pressure.

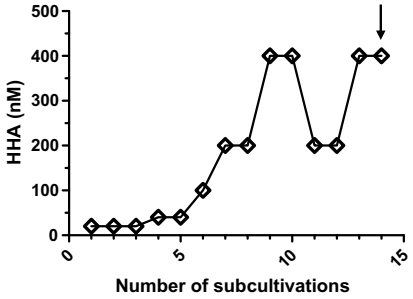

Virus	n	Asn67			Asn153		
WT	*5*	*N*	*T*	*T*	*N*	*D*	*T*
HHA^{res}	*14*	*D*	*T*	*T*	*N*	*D*	*I*
	1	*N*	*T*	*T*	*D*	*D*	*T*
	1	*N*	*T*	*I*	*N*	*D*	*I*
	1	*N*	*T*	*A*	*N*	*D*	*I*
	1	*N*	*T*	*T*	*N*	*D*	*I*

Fig. 1. Selection pathway for HHA resistant DENV-2 in mosquito C6/36 cells. The concentration of HHA was gradually increased during subcultivations. Every 3–4 days, subcultivation was performed by transferring a 1–20 dilution of the supernatant of HHA-exposed DENV-infected C6/36 cells to uninfected mosquito cells. At passage 14 (arrow), the virus was then collected and sequenced by population and clonal sequence analysis. Population sequence of HHA^{res} DENV revealed two mutations; N67D and T155I compared to the WT virus which was cultured in parallel for 14 passages in the absence of HHA. Clonal sequence of 5 WT and 18 HHA^{res} DENV clones revealed one or two mutations, in Asn67 and/or in Asn153 (n = number of clones sequenced).

Table 1
Primers for the amplification and sequencing of the structural proteins of DENV-2.

	Orientation	Nucleotide position	5′–3′ sequence
#491	Sense	1	GATGAGGGAAGATGGGGAGTTGTTAGTCTACGTGGAC
#492	Sense	1669	GCGAAGAAACAGGATGTTGTTG
#493	Sense	2182	GGTGACACAGCCTGGGATTT
#524	Antisense	2980	CCGCTGACATGAGTTTTGAGTC
#530	Antisense	1250	CATCCATTTCCCCATCCTCT
#531	Antisense	1763	TTTCCTGATGACATYTGGATTTC
#809	Sense	871	GGAACGACACATTTCCAAAGAG
#810	Antisense	1613	CACAAGGATCAAATTGGATACAG

2.7. Clonal sequencing of HHA^{res} DENV

For clonal sequencing, the gel-purified RT-PCR products (see above) were inserted into pJet1.2 (Clonejet Blunt-End Cloning System, Fermentas) and transformed in *Escherichia coli* top 10 cells (Invitrogen). 18 clones for HHA^{res} DENV and 5 clones for WT DENV were randomly selected and the respective plasmid DNA was sequenced with the DENV-2 specific primers #809 and #810 (Table 5.1). Sequence variation was assessed after multiple sequence alignments by the Vector NTI® software (Life Technologies, Merelbeke, Belgium).

2.8. Antiviral assays

A variety of cell types (Vero, BHK-21, Huh-7, Raji/DC-SIGN$^+$, Raji/L-SIGN$^+$ and MDDC)were seeded in a flat-bottom polystyrene 24 well-tray (Iwaki, International Medical Products, Belgium) and infected with WT or HHA^{res} DENV in the presence or absence of compound under the following conditions: 0.2×10^6 Vero cells/well were infected at a MOI of 0.005; 0.15×10^6 BHK-21 cells/well were infected at a MOI of 0.006; 0.05×10^6 Huh-7 cells/well were infected at a MOI of 0.02; 0.5×10^6 Raji/DC-SIGN$^+$ and Raji/L-SIGN$^+$ cells/well were infected at a MOI of 0.002; 1×10^6 MDDC/well were infected at a MOI of 0.0005. 2×10^6 C6/36 cells were seeded in T12.5 culture flasks (Falcon Becton Dickinson, Erembodegem, Belgium) and were infected at a MOI of 0.001 of WT or HHA^{res} DENV. After 4 h, the cells were washed twice with medium to remove excessive virus and compound and were further incubated at 37 °C in fresh culture medium. RBV and SA-17 were added again after the washing step to ensure antiviral activity of the compounds. Prior to infection, SA-17 was pre-incubated with the virus for 30 min at 37 °C (Kaptein et al., 2010). DENV infection was analyzed by flow cytometry, RT-qPCR and/or by confocal microscopy.

2.9. Flow cytometry analysis

Infection was quantified by means of (intracellular) flow cytometry as described previously (Alen et al., 2011). Viral infection was analyzed in Vero cells 7 days post infection, in BHK-21, Huh-7, C6/36, Raji/DC-SIGN$^+$ and Raji/L-SIGN$^+$ cells 4 days post infection and in MDDC 2 days post infection, because at these time points viral infection was optimal detected. Raji/DC-SIGN$^+$ and Raji/L-SIGN$^+$ cells were collected, washed with PBS supplemented with 2% FBS and stained with 5 μg/ml monoclonal anti-dengue virus antibody, recognizing the pre-membrane (prM) protein of all DENV serotypes (clone 2H2, Chemicon International/Millipore, Billerica, MA). After an incubation period of 30 min at room temperature, cells were washed with PBS and incubated with secondary PE-conjugated goat F(ab′)$_2$ anti-mouse antibody (1 μg/ml, Caltag Invitrogen Carlsbad, CA, USA) for 30 min at room temperature. Finally, the cells were washed with PBS and fixed with 1% formaldehyde.

Huh-7, BHK-21, Vero, C6/36 and MDDC were collected, washed with PBS, fixed and permeabilized using the Cytofix/Cytoperm Kit (BD Biosciences) according to the manufacturer's instructions. Cells were fixed and permeabilized with Cytofix/Cytoperm buffer at 4 °C for 20 min. After washing the cells with perm/wash buffer the permeabilized cells were incubated with 5 μg/ml anti-DENV mAb (clone 2H2) for 30 min at 4 °C. Following a washing step, the secondary PE-conjugated goat F(ab′)$_2$ anti-mouse Ab (Caltag Invitrogen) was added and incubated at 4 °C. As a control for unspecific background staining, cells were stained in parallel with secondary antibody only. The cells were then washed and analyzed by flow cytometry with a FACSCalibur (BD Biosciences, San Jose, CA). Data were acquired and analyzed with CellQuest software (BD Biosciences). The mean fluorescence of intensity (MFI) of the background staining was subtracted from the MFI of each sample to obtain the exact percentage of DENV-infected cells.

2.10. RNA extraction and RT-qPCR

Viral RNA was purified from the supernatant and quantified by RT-qPCR. Total RNA was extracted from 150 μl cell culture supernatant using the Nucleospin RNA Virus Kit according to the manufacturer's instructions (Macherey–Nagel, Düren, Germany). RT-qPCR was performed as described previously (Alen et al.,

2009). Briefly, the sequences of the forward (5′-TCGGAGCCGGAGT TTACAAA-3′ position 4628–4647) and reverse (5′-TCTTAACG TCCGCCATGAT-3′, position 4722–4741) Taqman primers were selected from non-structural gene 3 (NS3) of DENV NGC using Primer Express software (version 2.0, Applied Biosystems, Lennik, Belgium). The probe was selected between the primers and is fluorescently labeled with 6-carboxyfluorescein (FAM) at the 5′ end as the reporter dye and with a quencher at the 3′ end. The quencher is a minor groove binder (MGB) (5′-FAM-ATT-CCACACAATGTGGCA-MGB-3′, position 4656–4674). The nucleotide sequence and position of the primers and probes were obtained from the nucleotide sequence of DENV 2 NGC (GenBank accession No. M29095) (Irie et al., 1989). One step RT-qPCR was performed in a 25 μl reaction mixture containing 12.5 μl One-Step Reverse Transcriptase qPCR Master Mix (Eurogentec, Seraing, Belgium), 900 nM forward primer, 900 nM reverse primer, 200 nM probe and 100 ng sample RNA. RT-qPCR was performed under the following conditions: reverse transcription at 48 °C for 30 min, initial denaturation at 95 °C for 10 min, followed by 40 cycles of denaturation at 95 °C for 15 s, annealing and extension at 60 °C for 1 min. RT-qPCR was performed using the ABI 7500 Fast Real-Time PCR System (Applied Biosystems) and data were analyzed with ABI PRISM 7500 SDS software (version 1.3.1, Applied Biosystems). Standard curves were made of dengue virus plasmid with known concentrations to calculate the absolute quantification of infection.

2.11. Confocal microscopy

Huh-7 cells and Vero cells were infected with WT and HHA^{res} DENV and viral infection was visualized by confocal microscopy at respectively 4 and 7 days post infection. Cells were washed, fixated and incubated with anti-DENV antibodies as previously described (Alen et al., 2011). Briefly, cells were fixed with 3.7% formaldehyde for 15 min at room temperature and permeabilized with 0.1% Triton X-100 for 10 min at room temperature. After several washing steps, cells were incubated with 2% bovine serum albumin (BSA) (Sigma–Aldrich, St. Louis, MO, USA) in PBS. Next, cells were stained with anti-DENV mAb (clone 2H2) followed by incubation with a secondary antibody goat-anti-mouse IgG Alexa fluor 488 (Invitrogen). The cover slips were mounted with prolong gold anti-fade reagent and DAPI (Invitrogen) to stain the nucleus and incubated at 4 °C until the cells were processed for microscopic analysis. Images were collected with a Leica TCS SP5 laser scanning confocal microscope (Leica Microsystems, Mannheim, Germany) equipped with an AOBS, using a HCX PL APO 63.0x (NA:1.40) oil immersion lens. The different fluorochromes were detected sequentially using excitation lines of 405 nm (DAPI) and 488 nm (Alexa fluor 488). Emission was detected between 410–475 nm and 493–575 nm respectively.

2.12. Statistical analysis

Statistical analysis performed on the results included the calculation of the mean, standard error of the mean (SEM) and p-values by use of a two-tailed Student's t test. The significance level was set at $p < 0.05$. Statistical analysis was performed with GraphPad Prism statistical software (GraphPad Software, Inc., San Diego, CA).

3. Results

3.1. Selection of HHA^{res} DENV

To identify the specific molecular target epitopes of the CBAs on the DENV serotype 2 (DENV-2) envelope, we selected virus variants resistant to HHA in one selection experiment in the mosquito cell line C6/36. We choose for the C6/36 cells for the selection of the resistant virus because this cell line is highly permissive for DENV infection and is therefore commonly used to grow DENV stocks (Gubler,1998). HHA^{res} DENV was generated by adding a 1–20 dilution of the supernatant of HHA-exposed DENV-infected C6/36 mosquito cells every 3–4 days to fresh uninfected cells in the presence of gradually increasing concentrations of HHA. The drug resistance selection schedule is depicted in Fig. 1. After 14 passages (~7 weeks of cell culture), virus was recovered that replicated in the presence of 400 nM of HHA, that is at a concentration ~10-fold higher than the EC_{50} for inhibition of DENV-2 replication in C6/36 cells. At several passages (3, 6, 10, 14) the supernatant of the HHA-exposed DENV infected cells was analyzed for viral replication in Huh-7 cells by flow cytometry as described (Alen et al., 2009).

3.2. Genotypic analysis of HHA^{res} DENV

Two unique mutations were identified in the E-protein of the resistant virus analyzing the viral population after 14 passages: N67D and T155I (Fig. 1). No mutations were observed in the other structural proteins: the core protein or in the prM protein. The E protein of most flaviviruses contains at least one N-glycosylation motif $_{153}$N-D-T$_{155}$ (amino acid positions given as in the E-protein of DENV-2 NGC strain) and in the case of the four DENV serotypes also a second N-glycosylation motif $_{67}$N-T-T$_{69}$ (Bryant et al., 2007). The two mutations N67D and T155I observed are not compatible with the N-glycosylation sequence N-X-T/S (Ploegh and Neefjes, 1990) necessary to glycosylate the N in N-X-T/S. Thus, the observed mutations can be considered to result in the deletion of both N-glycans in the DENV E-glycoprotein. Clonal sequence analysis of HHA^{res} DENV revealed that in 80% (n = 14/18) of all HHA^{res} DENV clones (n = 18) sequenced both mutations, N67D and T155I were present. Two other mutations were identified in another two clones resulting in the deletion of the N-glycan on Asn67, namely T69I and T69A (each formally 5% (n = 1/18) of all HHA^{res} DENV clones). These clones also carried the second already observed mutation T155I. There were also clones with only one mutation either N153D or T155I resulting in a virus with one N-glycan deletion only on Asn153 (Fig. 1). None of the WT DENV clones (n = 5) derived from the control virus cell culture passaged in parallel displayed any mutations.

3.3. Phenotypic analysis of HHA^{res} DENV

Viral fitness of WT and HHA^{res} DENV were compared. First, we investigated the plaque phenotype in BHK-21 cell cultures of the mutant DENV and observed a smaller plaque phenotype for HHA^{res} DENV compared to the WT DENV (Fig. 2A). Next, Vero cells were infected with WT and HHA^{res} DENV at a MOI of 0.005. After 4 h of incubation, the input virus was removed and cells were washed twice with culture medium. The amount of viral RNA was quantified in the supernatants at different time points after infection. As shown in Fig. 2B, both WT and HHA^{res} DENV could replicate efficiently in Vero cells. Though HHA^{res} DENV showed a slightly slower growth relative to the WT DENV (i.e., an about 5-fold reduction) in Vero cells. Comparable data were obtained in BHK-21 cells (data not shown).

Third, a variety of cell types, mammalian and insect cells, were infected with WT and HHA^{res} DENV and the amount of infected cells was analyzed by flow cytometry using an anti-DENV antibody recognizing the prM protein of all serotypes of DENV (Fig. 3A). Viral replication and secretion seemed to be similarly efficient for WT and HHA^{res} DENV in Vero cells, as DENV Ag expression was detected equally strong for both viruses in Vero cells. Moreover, HHA^{res} DENV infected markedly more C6/36 cells if compared to

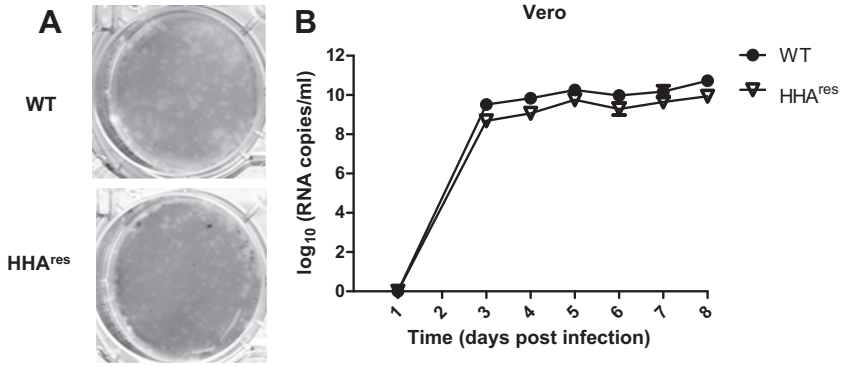

Fig. 2. (A) Plaque phenotype of WT and HHA^{res} DENV-2 was determined in BHK-21 cells 5 days post infection. (B) Viral replication efficiency of WT and HHA^{res} DENV-2 was evaluated time-dependently in Vero cells. Vero cells were infected at a MOI of 0.005. At the indicated time points, supernatants were collected and extracellular virus titers were determined by RT-qPCR. Data shown represent the mean ± SEM from 2 independent experiments performed in triplicate.

the WT DENV (Fig. 3A). In contrast, the mutant HHA^{res} DENV was only partially reduced in its capacity to replicate in hamster BHK-21 cells and human hepatoma (Huh-7) cells. Here at least 40% of the cells were infected by HHA^{res} DENV after 4 days as analyzed by flow cytometry (Fig. 3A). In summary, HHA^{res} DENV turned out to be if at all, only slightly reduced in its infectivity for a variety of mammalian and mosquito cells lacking DC-SIGN expression.

Remarkably, in contrast to WT DENV, HHA^{res} DENV was not able to efficiently infect DC-SIGN^{+} cells or cells that express the DC-SIGN-related liver-specific receptor L-SIGN (Fig. 3A). In addition, MDDC were also not susceptible for HHA^{res} DENV infection, corroborating the importance of the DC-SIGN-mediated DENV infection in MDDC.

Viral infection and replication of both WT and HHA^{res} DENV was confirmed by immunofluorescent microscopy monitoring the expression of DENV antigens in the cytosol of infected Huh-7 and Vero cells (Fig. 3B).

All together, these data indicate an efficient infection and production of infectious progeny of HHA^{res} DENV, lacking both glycosylation sites, in mammalian and insect cell lines with the considerable exception of DC-SIGN^{+} cells.

3.4. Cross-resistance profile of HHA^{res} DENV

The antiviral activity of several CBAs was investigated against the HHA^{res} and WT DENV in Huh-7 cells. Evaluation of the antiviral activity may be more relevant in human liver cells than in hamster (BHK-21) or monkey kidney cells (Vero) as the liver is considered to be an important target organ of DENV (Zellweger et al., 2010) and HHA^{res} DENV can replicate in this cell line (Fig. 3A). Huh-7 cells were infected with WT and HHA^{res} DENV in the absence or presence of different compounds. At four days post infection, the amount of infected cells was quantified by anti-DENV mAb clone 2H2 and by means of flow cytometry. Concentrations as high as 50-fold the EC_{50} of HHA against WT DENV did not inhibit HHA^{res} DENV entry in Huh-7 cells (Fig. 4 and Table 2).

HHA^{res} DENV was cross-resistant against the GNA lectin that as HHA recognizes α-1,3 mannose residues. UDA, which recognizes primarily the N-acetylglucosamine residues of N-glycans, also lacked antiviral activity against HHA^{res} DENV in Huh-7 cells. This indicates that the entire backbone of the N-glycan is deleted in line with the mutational pattern observed in the mutant E-proteins. Likewise, pradimicin-S (PRM-S), a small-size α-1,2-mannose-specific CBA, was also unable to inhibit HHA^{res} DENV. This demonstrates

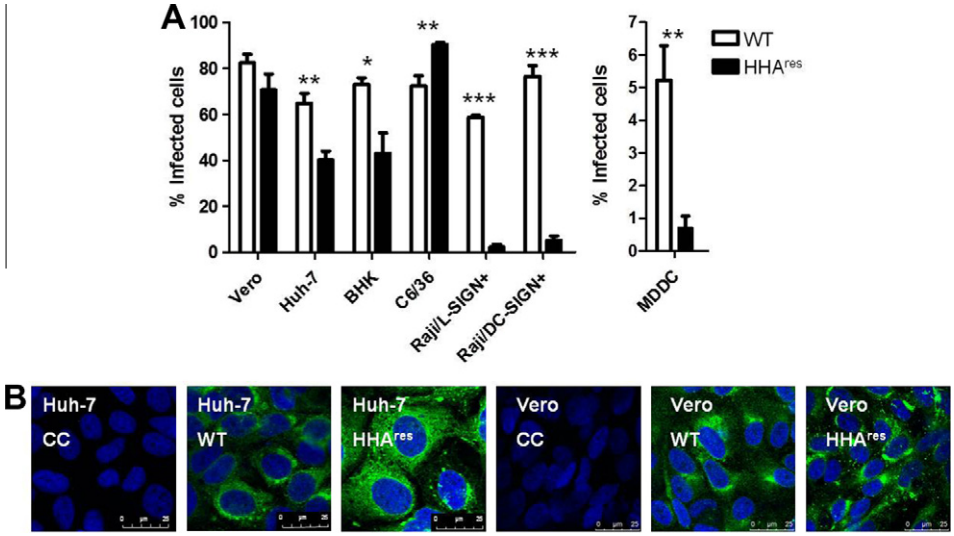

Fig. 3. Phenotypic analysis of HHA^{res} DENV-2 compared to WT DENV-2. (A) Various cell types were each infected at the same MOI of WT and HHA^{res} DENV. Infection was quantified by means of flow cytometry, using an anti-DENV antibody recognizing prM protein, clone 2H2. Mean % of infected cells ± SEM is shown for 2 independent experiments of duplicates. *p*-values were determined by a Students *t* test. Significance comparing WT and HHA^{res} DENV: $^{*}p < 0.05$; $^{**}p < 0.01$; $^{***}p < 0.001$. (B) Viral antigen expression in Huh-7 or Vero cells infected with either WT or HHA^{res} DENV was visualized by confocal microscopy images. Nuclei were stained with DAPI (blue). Infected cells were first incubated with anti-DENV antibody clone 2H2 and then with a goat-anti-mouse antibody labeled with Alexa fluor 488 (green).

that PRM-S targets also the glycans on the DENV envelope. In contrast, ribavirin (RBV), a nucleoside analog and inhibitor of cellular purine synthesis (Leyssen et al., 2008), retained as expected wild-type antiviral activity against HHA^{res} DENV. SA-17, a novel doxorubicin analog that inhibits the DENV entry process by another molecular mechanism of action than targeting viral N-glycans (Kaptein et al., 2010), was equipotent against WT DENV and HHA^{res} DENV.

Table 2
Antiviral activity of various CBAs, ribavirin and SA-17 against WT and HHAres DENV-2 in Huh-7 cells.

Compound	EC_{50}[a]	
	WT DENV-2	HHAres DENV-2
HHA (nM)	8.2 ± 4.6	>2000
GNA (nM)	9.4 ± 4.0	>2000
UDA (μM)	1.6 ± 0.57	>10
PRM-S (μM)	17 ± 3.7	>100
RBV (μM)	123 ± 22	107 ± 2.1
SA-17 (μM)	52 ± 20	44 ± 20

[a] EC_{50}, 50% effective concentration, or drug concentration required to inhibit DENV infection in Huh-7 cells by 50% as measured by viral antigen expression 4 days post infection. Values are the mean ± SEM of 2–5 independent experiments.

4. Discussion

Previously, we demonstrated a consistent and serotype-independent antiviral activity of the CBAs, HHA, GNA and UDA in Raji/DC-SIGN$^+$ cells and MDDC. Both cell types serve as *in vitro* models for DC that are considered to represent the first target cells of DENV in the human body (Grassi et al., 1998). Here, we characterized the molecular target of the CBAs on the viral envelope by the generation of a DENV resistant to HHA in the *Aedes albopictus* mosquito cell line C6/36. We succeeded in selecting a HHA^{res} DENV after 14 passages by gradually increasing the concentration of HHA (Fig. 1). Next, we characterized the genotype and the phenotype of the HHA^{res} virus. Compared with the WT DENV, we found two highly prevalent mutations, namely N67D and T155I, present in 80% of all HHA^{res} DENV clones sequenced. Similar mutational patterns destroying both glycosylation motifs (T69I or T69A each in combination with T155I) were each present in another 10% of the HHA^{res} DENV clones analyzed (Fig. 1). In 90% of the HHA^{res} DENV clones both N-glycosylation motifs were mutated either directly at the actual N-glycan accepting a residue of the first site (Asn67) or at the C-proximal Thr155 being an essential part of the second N-glycosylation site (Ploegh and Neefjes,1990), thus both N-glycosylation sites on the viral envelope protein can be considered to be deleted. This indicates that HHA directly targets the N-glycans on the viral E-protein. In fact, all HHA^{res} DENV clones sequenced showed the deletion of the N-glycan at Asn153. However, 10% ($n = 2/18$) of the HHA^{res} DENV clones sequenced had no mutation at the glycosylation motif $_{67}$N-T-T$_{69}$, indicating that this glycosylation motif (Mondotte et al., 2007) has a higher genetic barrier compared to $_{153}$N-D-T$_{155}$. Though there are multiple escape pathways to become resistant to HHA, but it seems not to be possible to fully escape the selective pressure of favoring a deglycosylation of the viral E-protein. In addition, we found no mutations either apart from the N-glycosylation sites of the E-protein discussed before, or in any of the five WT DENV-2 clones passaged in parallel. This is not fully unexpected as flaviviruses replicate with reasonable fidelity and DENV does not necessarily exist as a highly diverse quasispecies neither *in vitro* nor *in vivo* (Pugachev et al., 2004; Thai et al., 2012).

Then, the phenotype of HHA^{res} was characterized. According to the plaque assay in BHK-21 cells, HHA^{res} DENV had a smaller plaque phenotype compared to the WT DENV. These findings are in accordance with previous observations where mutant DENV with a deletion of the N-glycosylation site at N153 resulted in smaller plaques if compared with the WT virus (Lee et al., 1997; Mondotte et al., 2007). Previously, others demonstrated a loss of viral growth in mammalian cells when DENV lacks its glycosylation site at Asn67 (Mondotte et al., 2007; Bryant et al., 2007). Therefore, we investigated the viral fitness of the HHA^{res} virus in a variety of cell types. In contrast to these previous observations, we demonstrated a comparable viral growth in Vero cells for the mutant HHA^{res} and WT DENV analyzed by flow cytometry and RT-qPCR. We cannot formally exclude a reversion of HHA^{res} DENV back to WT DENV during growth in Huh-7 cells, however the latter seems highly unlikely given the rather short time frame of only 4 days used for

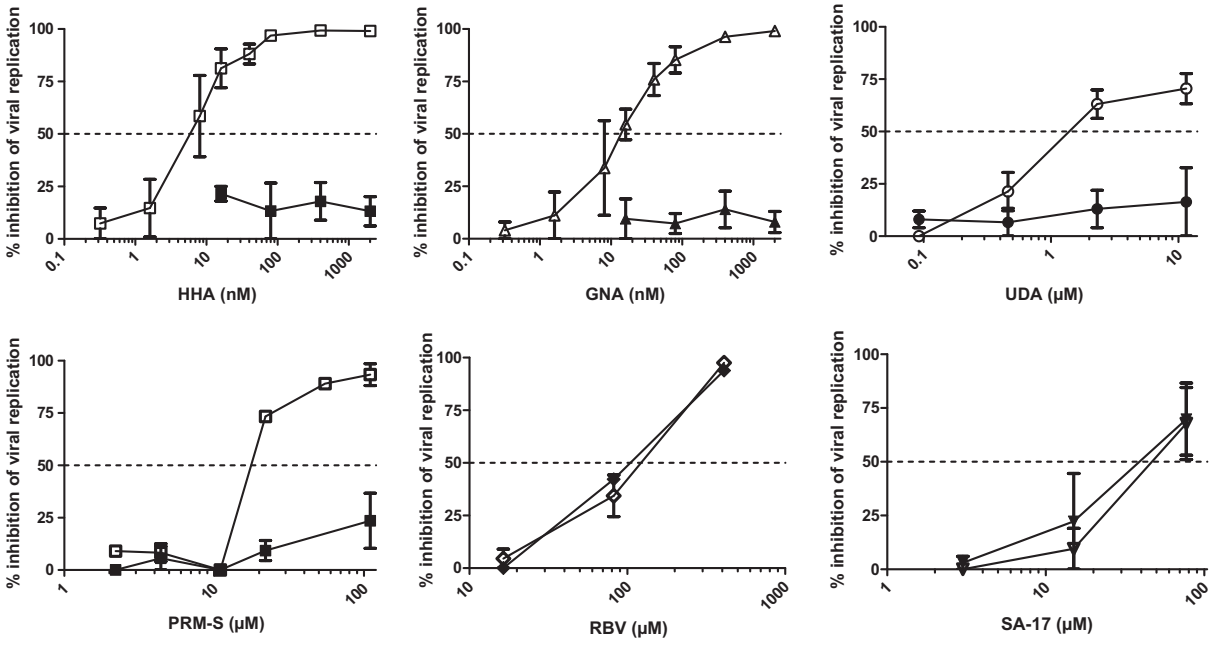

Fig. 4. HHA^{res} DENV-2 is cross-resistant to CBAs. Huh-7 cells were infected with WT (open symbol) or with HHA^{res} (black symbol) DENV at a MOI of 0.02 in the presence of various CBAs (HHA, GNA, UDA, PRM-S) or RBV or SA-17. At 4 days post infection, the number of DENV-infected cells was quantified by flow cytometry. The mean % of inhibition of viral replication ± SEM of up to 4 independent experiments is shown.

antiviral testing. Second, no WT DENV could be detected in the HHA^{res} DENV inoculums within the 18 representative clones analyzed making a rapid outgrowth of DENV variants almost impossible. In the C6/36 mosquito cells, the viral replication was even significantly higher for the HHA^{res} DENV. However, there was some kind of reduced viral fitness at least in a few cell lines tested. We observed that the mutant HHA^{res} DENV had a partially reduced replication capacity in hamster BHK-21 cells and human hepatoma (Huh-7) cells. A possible explanation for the differences between our data and data from previous studies could be that the mutant virus has been generated in mosquito C6/36 cells (during replication under antiviral drug pressure) and not in mammalian cells (after introducing the mutations by site-directed mutagenesis). In addition, in previous studies, other amino acid substitutions were generated, resulting in different virus genotypes and subsequently resulting in poorly to predict virus phenotypes. Lee et al. (2010) postulated that the virus fitness of mutant viruses lacking glycosylation sites is dependent on the viral strain and can be compensated by second-site amino acid mutations in the E-protein that can restore the virus growth in mammalian cells. According to our data, HHA^{res} DENV did not show additional compensatory amino acid mutations in that region.

Remarkably, in contrast to WT DENV, HHA^{res} DENV was not able to infect efficiently DC-SIGN^{+} cells or cells that express the DC-SIGN-related liver-specific receptor L-SIGN. Comparable data were previously obtained using another mutant DENV with deleted N-glycans (Pokidysheva et al., 2006; Mondotte et al., 2007). Our data indicate that the glycans present in the WT virus play a crucial role in the interaction with DC-SIGN and L-SIGN of the human host cell. Interestingly, MDDC are also not susceptible for HHA^{res} DENV infection, indicating the importance of the DC-SIGN-mediated DENV infection in MDDC. Moreover, cells of the hematopoietic origin, such as DC, have been shown to play a key role for DENV pathogenesis (Pham et al., 2012). Thus, if the CBA-resistant, N-glycan free DENV, cannot infect DC anymore we can assume that CBAs interfere with a pathophysiological highly relevant target. By contrast, the entry process of DENV in Vero, Huh-7, BHK-21 and C6/36 cell lines is DC-SIGN-independent and also carbohydrate-independent. Indeed, HHA^{res} DENV can enter and replicate in these cell lines. In fact, we demonstrate here for the first time that DENV that lacks N-glycans on the envelope E-glycoprotein is able to replicate efficiently in mammalian cells, with the exception of DC-SIGN^{+} cells.

The HHA^{res} virus was used as a tool to identify the antiviral target of other classes of compounds as it could replicate in human liver Huh-7 cells (Fig. 3A). The HHA^{res} DENV was cross-resistant to GNA, UDA and PRM-S because these compounds recognize different molecules present in the structure of an N-glycan. In contrast, ribavirin (RBV), a nucleoside analog and inhibitor of cellular purine synthesis (Leyssen et al., 2008), retained as expected wild-type antiviral activity against HHA^{res} DENV. This argues against that there would be relevant compensatory mutations e.g., in the non-structural proteins of DENV which might be responsible for an overall enhanced replication of the viral genome as shown for other inhibitors of DENV replication (Xie et al., 2011; Wang et al., 2011). SA-17, a novel doxorubicin analog that inhibits the DENV entry process (Kaptein et al., 2010), was equipotent against WT and HHA^{res} DENV. The SA-17 compound is predicted to interact with the hydrophobic binding pocket of the E-glycoprotein which is independent from the N-glycosylation state of the E-glycoprotein and this hypothesis was confirmed by molecular docking experiments (Kaptein et al., 2010).

5. Conclusion

In conclusion, we generated a HHA^{res} DENV-2 strain that apparently in cells lacking DC-SIGN has a comparable fitness as WT DENV. However, DC-SIGN expressing cells were markedly less susceptible to HHA^{res} DENV, indicating a crucial role of the E-glycoprotein N-glycans for DC-SIGN-mediated DENV infection. MDDC could not become infected with HHA^{res} DENV, indicating that DENV is dependent on N-glycans for establishing an infection at its primary inoculation site in the human skin. Thus, based on this study, DC-SIGN expressing cells can be considered as a "bottleneck" for DENV pathogenesis. Moreover, in line with the crucial role that DC-SIGN plays in DENV pathogenesis (Sakuntabhai et al., 2005), DENV N-glycan deletion mutants should most probably have an attenuated phenotype *in vivo* and could possibly be used in novel vaccination strategies. In addition, the HHA^{res} DENV can be considered as demonstrated in this study as a useful tool in order to elucidate target specificity (i.e., glycans on DENV E-glycoprotein) of novel viral entry inhibitors.

Acknowledgements

This work was supported by the FWO (G-485-08 and G.0528.12N), the KU Leuven (PF/10/018 and GOA/10/014) and the EU FP7 Project CHAARM (No. 242135). We are thankful to E. Vanstreels, S. Claes, B. Provinciael, E. Van Kerckhove and E. Fonteyn for excellent technical assistance.

References

Alen, M.M.F., De Burghgraeve, T., Kaptein, S.J.F., Balzarini, J., Neyts, J., Schols, D., 2011. Broad antiviral activity of carbohydrate-binding agents against the four serotypes of dengue virus in monocyte-derived dendritic cells. Plos One 6, e21658.

Alen, M.M.F., Kaptein, S.J.F., De Burghgraeve, T., Balzarini, J., Neyts, J., Schols, D., 2009. Antiviral activity of carbohydrate-binding agents and the role of DC-SIGN in dengue virus infection. Virology 387, 67–75.

Balzarini, J., Van Herrewege, Y., Vermeire, K., Vanham, G., Schols, D., 2007. Carbohydrate-binding agents efficiently prevent dendritic cell-specific intercellular adhesion molecule-3-grabbing nonintegrin (DC-SIGN)-directed HIV-1 transmission to T lymphocytes. Mol. Pharmacol. 71, 3–11.

Bryant, J.E., Calvert, A.E., Mesesan, K., Crabtree, M.B., Volpe, K.E., Silengo, S., Kinney, R.M., Huang, C.Y.H., Miller, B.R., Roehrig, J.T., 2007. Glycosylation of the dengue 2 virus E protein at N67 is critical for virus growth in vitro but not for growth in intrathoracically inoculated *Aedes aegypti* mosquitoes. Virology 366, 415–423.

Christenbury, J.G., Aw, P.P.K., Ong, S.H., Schreiber, M.J., Chow, A., Gubler, D.J., Vasudevan, S.G., Ooi, E.E., Hibberd, M.L., 2010. A method for full genome sequencing of all four serotypes of the dengue virus. J. Virol. Methods 169, 202–206.

Geijtenbeek, T.B.H., Kwon, D.S., Torensma, R., van Vliet, S.J., van Duijnhoven, G.C.F., Middel, J., Cornelissen, I.L.M.H., Nottet, H.S.L.M., KewalRamani, V.N., Littman, D.R., Figdor, C.G., van Kooyk, Y., 2000. DC-SIGN, a dendritic cell-specific HIV-1-binding protein that enhances trans-infection of T cells. Cell 100, 587–597.

Grassi, F., Dezutter-Dambuyant, C., McIlroy, D., Jacquet, C., Yoneda, K., Imamura, S., Boumsell, L., Schmitt, D., Autran, B., Debré, P., Hosmalin, A., 1998. Monocyte-derived dendritic cells have a phenotype comparable to that of dermal dendritic cells and display ultrastructural granules distinct from Birbeck granules. J. Leukoc. Biol. 64, 484–493.

Gubler, D.J., 1998. Dengue and dengue hemorrhagic fever. Clin. Microbiol. Rev. 11, 480–496.

Irie, K., Mohan, P.M., Sasaguri, Y., Putnak, R., Padmanabhan, R., 1989. Sequence-analysis of cloned dengue virus type-2 genome (New-guinea-C strain). Gene 75, 197–211.

Kaptein, S.J.F., De Burghgraeve, T., Froeyen, M., Pastorino, B., Alen, M.M.F., Mondotte, J.A., Herdewijn, P., Jacobs, M., de Lamballerie, X., Schols, D., Gamarnik, A.V., Sztaricskai, F., Neyts, J., 2010. A derivate of the antibiotic doxorubicin is a selective inhibitor of dengue and yellow fever virus replication in vitro. Antimicrob. Agents Chemother. 54, 5269–5280.

Lee, E., Leang, S.K., Davidson, A., Lobigs, M., 2010. Both E protein glycans adversely affect dengue virus infectivity but are beneficial for virion release. J. Virol. 84, 5171–5180.

Lee, E., Weir, R.C., Dalgarno, L., 1997. Changes in the dengue virus major envelope protein on passaging and their localization on the three-dimensional structure of the protein. Virology 232, 281–290.

Leyssen, P., De Clercq, E., Neyts, J., 2008. Molecular strategies to inhibit the replication of RNA viruses. Antiviral Res. 78, 9–25.

Lozach, P.Y., Burleigh, L., Staropoli, I., Navarro-Sanchez, E., Harriague, J., Virelizier, J.L., Rey, F.A., Desprès, P., Arenzana-Seisdedos, F., Amara, A., 2005. Dendritic cell-specific intercellular adhesion molecule 3-grabbing non-integrin (DC-SIGN)-mediated enhancement of dengue virus infection is independent of DC-SIGN internalization signals. J. Biol. Chem. 280, 23698–23708.

Matrosovich, M., Matrosovich, T., Garten, W., Klenk, H.D., 2006. New low-viscosity overlay medium for viral plaque assays. Virol. J. 3, 63–69.
Modis, Y., Ogata, S., Clements, D., Harrison, S.C., 2003. A ligand-binding pocket in the dengue virus envelope glycoprotein. Proc. Natl. Acad. Sci. USA 100, 6986–6991.
Mondotte, J.A., Lozach, P.Y., Amara, A., Gamarnik, A.V., 2007. Essential role of dengue virus envelope protein N-glycosylation at asparagine-67 during viral propagation. J. Virol. 81, 7136–7148.
Navarro-Sanchez, E., Altmeyer, R., Amara, A., Schwartz, O., Fieschi, F., Virelizier, J.L., Arenzana-Seisdedos, F., Desprès, P., 2003. Dendritic-cell-specific ICAM3-grabbing non-integrin is essential for the productive infection of human dendritic cells by mosquito-cell-derived dengue viruses. Embo. Rep. 4, 723–728.
Pham, A.M., Langlois, R.A., TenOever, B.R., 2012. Replication in cells of hematopoietic origin is necessary for dengue virus dissemination. Plos Pathog. 8, e1002465.
Ploegh, H., Neefjes, J.J., 1990. Protein glycosylation. Curr. Opin. Cell Biol. 2, 1125–1130.
Pöhlmann, S., Baribaud, F., Lee, B., Leslie, G.J., Sanchez, M.D., Hiebenthal-Millow, K., Munch, J., Kirchhoff, F., Doms, R.W., 2001. DC-SIGN interactions with human immunodeficiency virus type 1 and 2 and simian immunodeficiency virus. J. Virol. 75, 4664–4672.
Pokidysheva, E., Zhang, Y., Battisti, A.J., Bator-Kelly, C.M., Chipman, P.R., Xiao, C.A., Gregorio, G.G., Hendrickson, W.A., Kuhn, R.J., Rossmann, M.G., 2006. Cryo-EM reconstruction of dengue virus in complex with the carbohydrate recognition domain of DC-SIGN. Cell 124, 485–493.
Pugachev, K.V., Guirakhoo, F., Ocran, S.W., Mitchell, F., Parsons, M., Penal, C., Girakhoo, S., Pougatcheva, S.O., Arroyo, J., Trent, D.W., Monath, T.P., 2004. High fidelity of yellow fever virus RNA polymerase. J. Virol. 78, 1032–1038.
Rey, F.A., Heinz, F.X., Mandl, C., Kunz, C., Harrison, S.C., 1995. The envelope glycoprotein from tick-borne encephalitis virus at 2 angstrom resolution. Nature 375, 291–298.
Rodenhuis-Zybert, I.A., Wilschut, J., Smit, J.M., 2010. Dengue virus life cycle: viral and host factors modulating infectivity. Cell Mol. Life Sci. 67, 2773–2786.
Saitoh, K., Tsuno, T., Kakushima, M., Hatori, M., Furumai, T., Oki, T., 1993. Pradimicin-S, a new pradimicin analog. II. Isolation and structure elucidation. J. Antibiot. 46, 406–411.
Sakuntabhai, A., Turbpaiboon, C., Casademont, I., Chuansumrit, A., Lowhnoo, T., Kajaste-Rudnitski, A., Kalayanarooj, S.M., Tangnararatchakit, K., Tangthawornchaikul, N., Vasanawathana, S., Chaiyaratana, W., Yenchitsomanus, P.T., Suriyaphol, P., Avirutnan, P., Chokephaibulkit, K., Matsuda, F., Yoksan, S., Jacob, Y., Lathrop, G.M., Malasit, P., Desprès, P., Julier, C., 2005. A variant in the CD209 promoter is associated with severity of dengue disease. Nat. Genet. 37, 507–513.
Scherret, J.H., Mackenzie, J.S., Khromykh, A.A., Hall, R.A., 2001. Biological significance of glycosylation of the envelope protein of Kunjin virus. Ann. NY. Acad. Sci. 951, 361–363.
Seneviratne, S.L., Malavige, G.N., de Silva, H.J., 2006. Pathogenesis of liver involvement during dengue viral infections. Trans. R. Soc. Trop. Med. Hyg. 100, 608–614.
Sztaricskai, F., Sum, A., Roth, E., Pelyvas, I.F., Sandor, S., Batta, G., Herczegh, P., Reményi, J., Miklan, Z., Hudecz, F., 2005. A new class of semisynthetic anthracycline glycoside antibiotics incorporating a squaric acid moiety. J. Antibiot. 58, 704–714.
Tassaneetrithep, B., Burgess, T.H., Granelli-Piperno, A., Trumpfherer, C., Finke, J., Sun, W., Eller, M.A., Pattanapanyasat, K., Sarasombath, S., Birx, D.L., Steinman, R.M., Schlesinger, S., Marovich, M.A., 2003. DC-SIGN (CD209) mediates dengue virus infection of human dendritic cells. J. Exp. Med. 197, 823–829.
Thai, K.T.D., Henn, M.R., Zody, M.C., Tricou, V., Nguyet, N.M., Charlebois, P., Lennon, N.J., Green, L., de Vries, P.J., Hien, T.T., Farrar, J., van Doorn, H.R., de Jong, M.D., Birren, B.W., Holmes, E.C., Simmons, C.P., 2012. High-resolution analysis of intrahost genetic diversity in dengue virus serotype 1 infection identifies mixed infections. J. Virol. 86, 835–843.
Van Damme, E., Allen, A., Peumans, W., 1987. Isolation and characterization of a lectin with exclusive specificity towards mannose from snowdrop (*Galanthus nivalis*) bulbs. FEBS Lett. 251, 140–144.
Van Damme, E., Kaku, H., Perini, F., Goldstein, I., Peeters, B., Yagi, F., Decock, B., Peumans, W., 1991. Biosynthesis, primary structure and molecular cloning of snowdrop (*Galanthus Nivalis* L.) lectin. Eur. J. Biochem. 202, 23–30.
Vigerust, D.J., Shepherd, V.L., 2007. Virus glycosylation: role in virulence and immune interactions. Trends Microbiol. 15, 211–218.
Wang, Q.Y., Bushell, S., Qing, M., Xu, H.Y., Bonavia, A., Nunes, S., Zhou, J., Poh, M.K., de Sessions, P.F., Niyomrattanakit, P., Dong, H., Hoffmaster, K., Goh, A., Nilar, S., Schul, W., Jones, S., Kramer, L., Compton, T., Shi, P.Y., 2011. Inhibition of dengue virus through suppression of host pyrimidine biosynthesis. J. Virol. 85, 6548–6556.
Wu, S.J.L., Grouard-Vogel, G., Sun, W., Mascola, J.R., Brachtel, E., Putvatana, R., Louder, M.K., Filgueira, L., Marovich, M.A., Wong, H.K., Blauvelt, A., Murphy, G.S., Robb, M.L., Innes, B.L., Birx, D.L., Hayes, C.G., Frankel, S.S., 2000. Human skin Langerhans cells are targets of dengue virus infection. Nat. Med. 6, 816–820.
Xie, X., Wang, Q.Y., Xu, H.Y., Qing, M., Kramer, L., Yuan, Z., Shi, P.Y., 2011. Inhibition of dengue virus by targeting viral NS4B protein. J. Virol. 85, 11183–11195.
Zellweger, R.M., Prestwood, T.R., Shresta, S., 2010. Enhanced infection of liver sinusoidal endothelial cells in a mouse model of antibody-induced severe dengue disease. Cell Host Microbe 7, 128–139.